Hadronic contributions to $g-2$ from lattice QCD

Jeremy Green

NIC, DESY, Zeuthen

Second annual symposium
Helmholtz Programme "Matter and the Universe"
December 12–13, 2016

Outline

1. Brief overview of lattice activities at DESY
2. Introduction — muon $g-2$
3. Hadronic vacuum polarization
4. Hadronic light-by-light scattering
5. Outlook

Lattice QCD

…is a regularization of Euclidean-space QCD such that the path integral can be done fully non-perturbatively.

- Euclidean spacetime becomes a periodic hypercubic lattice, with spacing a and box size $L_s^3 \times L_t$.
- Path integral over fermion degrees of freedom is done analytically, for each gauge configuration. Solving the Dirac equation with a fixed source yields a source-to-all quark propagator.
- Path integral over gauge degrees of freedom is done numerically using Monte Carlo methods to generate an *ensemble* of *gauge configurations*.

The $a \to 0$ and $L_s, L_t \to \infty$ extrapolations need to be taken by using multiple ensembles.

Lattice activities at DESY

- Broad research in lattice field theory
  - lattice QCD
  - algorithm and conceptual developments
  - new approaches (e.g. tensor network techniques)
- Multi-level algorithm → reduce exponential signal-to-noise problem
- Group plays leading and central role in two large European efforts:
  - European Twisted Mass Collaboration (ETMC)
  - Coordinated Lattice Simulations (CLS)

ALPHA Collaboration:

- HQET, B-physics
- final determination of strong coupling constant based on 3-flavour calculations
- lattice ensembles pushing toward physical quark masses

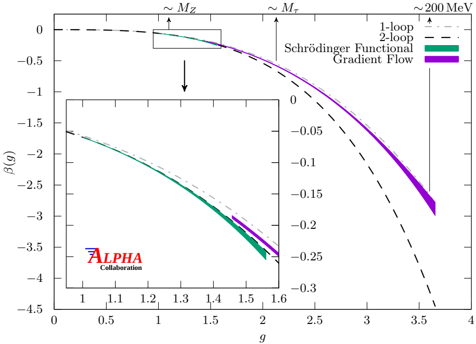

Lattice activities at DESY

ETMC:

- Nucleon sigma terms
  - computed on one $N_f = 2$ ensemble with physical m_π
  - relevant for dark matter searches
  - most precise results for σ_s and σ_c

Phys. Rev. Lett. **116**, 252001 (2016), 1601.01624

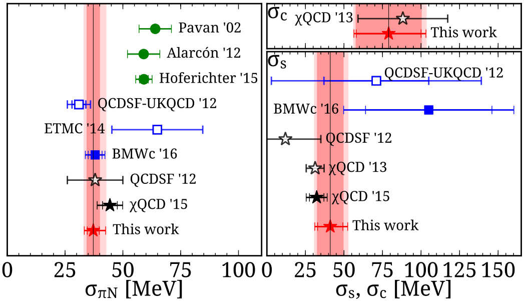

- Nucleon structure:
  - form factors
  - moments of parton distribution functions
  - direct calculation of parton distribution functions
- Muon anomalous magnetic moment
- Future outlook: more-physical calculations
  - $N_f = 2 + 1 + 1$ with correct π, K and D meson masses
  - include QED and isospin breaking

Muon anomalous magnetic moment

A muon has magnetic moment $\vec{\mu} = g_\mu \frac{e}{2m_\mu}\vec{S}$. The Dirac equation predicts $g_\mu = 2$, but quantum effects produce a small deviation,

$$a_\mu \equiv \frac{g_\mu - 2}{2} = \begin{cases} 116\,592\,089(63) \times 10^{-11} & \text{experiment BNL E821, PRD } \mathbf{73}\text{, 072003 (2006)} \\ 116\,591\,828(50) \times 10^{-11} & \text{theory US "Snowmass" Self Study, 1311.2198} \end{cases}$$

$\Delta a_\mu = (261 \pm 78) \times 10^{-11}$, a 3σ discrepancy.

- New experiments promise to reduce the uncertainty fourfold:
  - Fermilab E989, using the same storage ring from BNL.
  - J-PARC E34, using a new method with ultra-cold muons.
- The theoretical uncertainty should likewise be reduced.
  - Hadronic effects are the dominant contributions.

Muon $g-2$: theory uncertainty

The two dominant sources of uncertainty are hadronic effects:

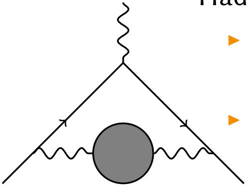

Hadronic vacuum polarization: $a_\mu^{\text{HVP,LO}} = 6949(43) \times 10^{-11}$.

- Determined using experimental data on cross section for $e^+e^- \to$ hadrons.
- Very active field for lattice QCD calculations working toward an *ab initio* prediction with competitive uncertainty.

Hadronic light-by-light scattering:
$a_\mu^{\text{HLbL}} = 105(26)$ or $116(39) \times 10^{-11}$.

- Determined using models that include meson exchange terms, charged meson loops, etc.
- Could benefit significantly with reliable input from the lattice.

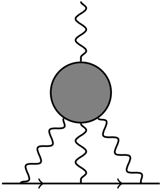

Hadronic vacuum polarization (HVP) on the lattice

$$a_\mu^{\text{HVP,LO}} = \left(\frac{\alpha}{\pi}\right)^2 \int_0^\infty dQ^2 f(Q^2) \left[\Pi(Q^2) - \Pi(0)\right],$$

where $f(Q^2)$ is a known kernel and the integrand peaks near $Q^2 = (m_\mu/2)^2$.
Two main strategies:

1. Momentum space

$$\Pi_{\mu\nu}(Q) \equiv \int d^4x\, e^{iQ\cdot x} \langle J_\mu(x) J_\nu(0)\rangle$$
$$= \left(g_{\mu\nu}Q^2 - Q_\mu Q_\nu\right)\Pi(Q^2)$$

Cannot directly obtain $\Pi(0)$.
Limited resolution at low Q^2, where $f(Q^2)$ is peaked, so constrained fitting is needed.

2. Time-momentum representation
D. Bernecker and H. B. Meyer,
Eur. Phys. J. A **47**, 148 (2011)

$$G(x_0) \equiv -\frac{1}{3}\sum_{k=1}^{3}\int d^3x\, \langle J_k(x_0,x) J_k(0)\rangle,$$

$$\Pi(Q^2) - \Pi(0) = \int_0^\infty dx_0 G(x_0) x_0^2 g(Qx_0),$$

$$g(y) \equiv 1 - \tfrac{4}{y^2}\sin^2(y/2)$$

Challenge is understanding large-x_0 behaviour of $G(x_0)$.

Timelike pion form factor

The time-momentum correlator has a spectral representation,

$$G(x_0) = \int_0^\infty d\omega\, \omega^2 \rho(\omega^2) e^{-\omega|x_0|}, \qquad \rho(s) = \frac{1}{12\pi^2} \frac{\sigma(e^+e^- \to \text{hadrons})}{4\pi\alpha(s)^2/(3s)}.$$

At low energies, this is given by $\sigma(e^+e^- \to \pi^+\pi^-)$, which depends on the timelike pion form factor $|F_\pi(\sqrt{s})|^2$. For $2m_\pi \le \sqrt{s} \le 4m_\pi$, this can be computed from finite-volume energy levels and matrix elements.

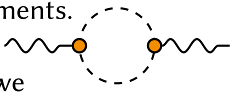

H. B. Meyer, Phys. Rev. Lett. **107**, 072002 (2011)

By separately computing $|F_\pi|^2$ and fitting it with a curve, we can replace the discrete low-energy finite-volume spectrum in $G(x_0)$ with a $\pi^+\pi^-$ continuum, and improve the approach to the infinite-volume limit.

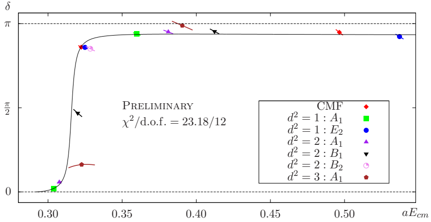

First step: compute the p-wave $\pi\pi$ scattering phase shift. Exploratory study with $m_\pi = 437$ MeV.

F. Erben, JG, D. Mohler, H. Wittig, poster at Lattice 2016, 1611.06805

Hadronic contributions to the muon $g-2$

$O(\alpha^2)$:
Leading order hadronic vacuum polarization.

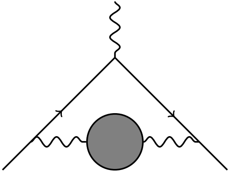

$O(\alpha^3)$:

Higher-order contributions from leading order HVP.

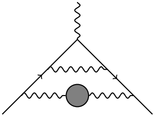

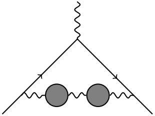

Leading-order contribution from $O(\alpha)$ correction to HVP.

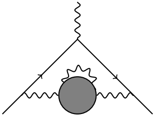

Included in the phenomenological leading-order HVP.

Hadronic light-by-light.

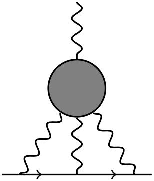

π^0 contribution to HLbL scattering

About 2/3 of theory prediction for a_μ^{HLbL} comes from π^0 exchange diagrams, which dominate at long distances. Large contributions also come from η, η'.

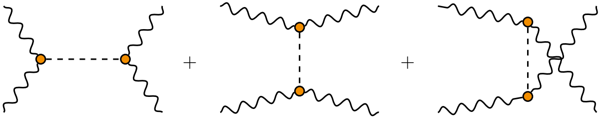

Their contribution to the four-point function:

$$\Pi^{E,\pi^0}_{\mu_1\mu_2\mu_3\mu_4}(p_4;p_1,p_2) = -p_{1\alpha}p_{2\beta}p_{3\sigma}p_{4\tau}\Bigg(\frac{\mathcal{F}_{12}\epsilon_{\mu_1\mu_2\alpha\beta}\mathcal{F}_{34}\epsilon_{\mu_3\mu_4\sigma\tau}}{(p_1+p_2)^2+m_\pi^2} + \frac{\mathcal{F}_{13}\epsilon_{\mu_1\mu_3\alpha\sigma}\mathcal{F}_{24}\epsilon_{\mu_2\mu_4\beta\tau}}{(p_1+p_3)^2+m_\pi^2} + \frac{\mathcal{F}_{14}\epsilon_{\mu_1\mu_4\alpha\tau}\mathcal{F}_{23}\epsilon_{\mu_2\mu_3\beta\sigma}}{(p_2+p_3)^2+m_\pi^2}\Bigg),$$

where $p_3 = -(p_1+p_2+p_4)$ and $\mathcal{F}_{ij} = \mathcal{F}(-p_i^2,-p_j^2)$ is the $\pi^0\gamma^*\gamma^*$ form factor.

Lattice calculation of the $\pi^0 \to \gamma^*\gamma^*$ form factor

A. Gérardin, H. B. Meyer, A. Nyffeler, Phys. Rev. D **94**, 074507 (2016), 1607.08174

In Minkowski space:

$$M_{\mu\nu}(p,q_1) = i \int d^4x \, e^{iq_1 x} \langle 0|T\{J_\mu(x) J_\nu(0)\}|\pi^0(p)\rangle = \epsilon_{\mu\nu\alpha\beta} q_1^\alpha q_2^\beta \mathcal{F}_{\pi^0\gamma^*\gamma^*}(q_1^2, q_2^2),$$

where $p = q_1 + q_2$. In Euclidean space on the lattice, compute

$$M_{\mu\nu}^E \equiv - \int d\tau \, e^{\omega_1 \tau} \int d^3z \, e^{-i\vec{q}_1 \vec{z}} \langle 0|T\{J_\mu(\vec{z},\tau) J_\nu(\vec{0},0)\}|\pi(p)\rangle.$$

Different models were fit to the lattice data, of which only LMD+V has the correct behaviour at large Q^2 of $\mathcal{F}(-Q^2,0)$ and $\mathcal{F}(-Q^2,-Q^2)$.

A. Gérardin, H. B. Meyer, A. Nyffeler, Phys. Rev. D **94**, 074507 (2016), 1607.08174

Doubly virtual (on one ensemble)

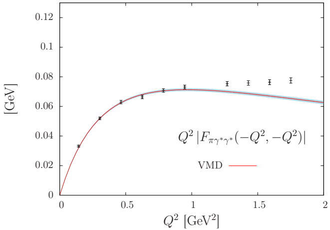

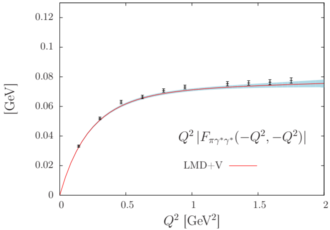

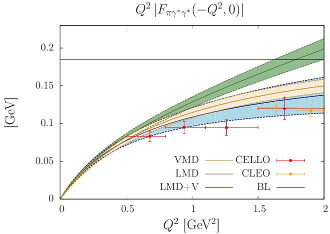

Singly virtual (extrapolated to m_π^{phys}, $a = 0$)

Preferred LMD+V fit model used to estimate the π^0 exchange contribution to $g-2$:

$$a_\mu^{\text{HLbL},\pi^0} = (65.0 \pm 8.3) \times 10^{-11},$$

which fits well into the range of model calculations, $(50-80) \times 10^{-11}$.

Light-by-light scattering

Before computing a_μ^{HLbL}, start by studying light-by-light scattering by itself.

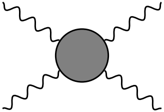

This has much more information than just a_μ^{HLbL}. We can:

- Compare against phenomenology.
- Test models used to compute a_μ^{HLbL}.

Some of these results were published in

JG, O. Gryniuk, G. von Hippel, H. B. Meyer, V. Pascalutsa, Phys. Rev. Lett. **115**, 222003 (2015) [1507.01577]

Quark contractions for four-point function

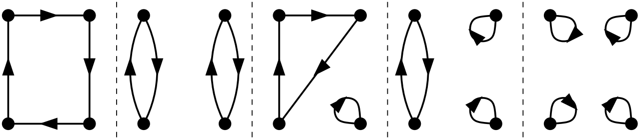

Compute only the *fully-connected* contractions, with fixed kernels summed over x_1 and x_2:

$$\Pi^{\text{pos}'}_{\mu_1\mu_2\mu_3\mu_4}(x_4; f_1, f_2) = \sum_{x_1,x_2} f_1(x_1) f_2(x_2) \left\langle J_{\mu_1}(x_1) J_{\mu_2}(x_2) J_{\mu_3}(0) J_{\mu_4}(x_4) \right\rangle$$

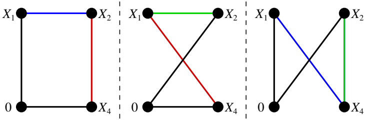

Generically, need the following propagators:

- 1 point-source propagator from $x_3 = 0$
- 8 sequential propagators through x_1, for each μ_1 and f_1 or f_1^*
- 8 sequential propagators through x_2
- 32 double-sequential propagators through x_1 and x_2, for each (μ_1, μ_2) and (f_1, f_2) or (f_1^*, f_2^*)

Kinematical setup

Obtain momentum-space Euclidean four-point function using plane waves:

$$\Pi^{E}_{\mu_1\mu_2\mu_3\mu_4}(p_4; p_1, p_2) = \sum_{x_4} e^{-ip_4\cdot x_4}\Pi^{\text{pos}'}_{\mu_1\mu_2\mu_3\mu_4}(x_4; f_1, f_2)\Big|_{f_a(x)=e^{-ip_a\cdot x}}.$$

Thus, we can efficiently fix $p_{1,2}$ and choose arbitrary p_4.

- Full 4-point tensor is very complicated: it can be decomposed into 41 scalar functions of 6 kinematic invariants.
- Forward case is simpler:

$$Q_1 \equiv p_2 = -p_1, \quad Q_2 \equiv p_4.$$

  Then there are 8 scalar functions that depend on 3 kinematic invariants.

Forward LbL amplitude

Take the amplitude for forward scattering of transversely polarized virtual photons,

$$\mathcal{M}_{TT}(-Q_1^2, -Q_2^2, \nu) = \frac{e^4}{4} R_{\mu_1\mu_2} R_{\mu_3\mu_4} \Pi^E_{\mu_1\mu_2\mu_3\mu_4}(-Q_2; -Q_1, Q_1),$$

where $\nu = -Q_1 \cdot Q_2$ and $R_{\mu\nu}$ projects onto the plane orthogonal to Q_1, Q_2.

A subtracted dispersion relation at fixed spacelike Q_1^2, Q_2^2 relates this to the $\gamma^*\gamma^* \to$ hadrons cross sections $\sigma_{0,2}$:

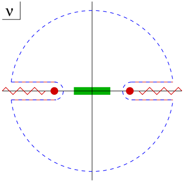

$$\mathcal{M}_{TT}(q_1^2, q_2^2, \nu) - \mathcal{M}_{TT}(q_1^2, q_2^2, 0) = \frac{2\nu^2}{\pi} \int_{\nu_0}^{\infty} d\nu' \frac{\sqrt{\nu'^2 - q_1^2 q_2^2}}{\nu'(\nu'^2 - \nu^2 - i\epsilon)} \left[\sigma_0(\nu') + \sigma_2(\nu')\right]$$

This is model-independent and will allow for systematically improvable comparisons between lattice and experiment.

Model for $\sigma(\gamma^*\gamma^* \to \text{hadrons})$

V. Pascalutsa, V. Pauk, M. Vanderhaeghen, Phys. Rev. D **85** (2012) 116001

Include single mesons and $\pi^+\pi^-$ final states:

$$\sigma_0 + \sigma_2 = \sum_M \sigma(\gamma^*\gamma^* \to M) + \sigma(\gamma^*\gamma^* \to \pi^+\pi^-)$$

Mesons:

- pseudoscalar (π^0, η')
- scalar (a_0, f_0)
- axial vector (f_1)
- tensor (a_2, f_2)

$\sigma(\gamma^*\gamma^* \to M)$ depends on the meson's:

- mass m and width Γ
- two-photon decay width $\Gamma_{\gamma\gamma}$
- two-photon transition form factor $F(q_1^2, q_2^2)$

assume $F(q_1^2, q_2^2) = F(q_1^2, 0)F(0, q_2^2)/F(0, 0)$

Use scalar QED dressed with form factors for $\sigma(\gamma^*\gamma^* \to \pi^+\pi^-)$.

$\mathcal{M}_{TT}$: dependence on ν and Q_2^2

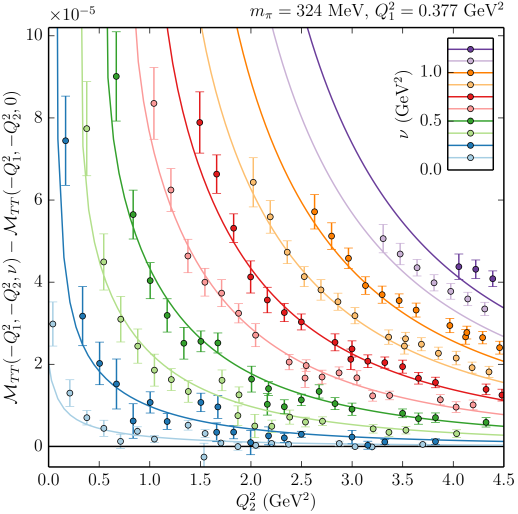

For scalar, tensor mesons there is no data from expt; we use

$$F(q^2, 0) = F(0, q^2) = \frac{1}{1 - q^2/\Lambda^2}$$

with Λ set by hand to 1.6 GeV

Changing Λ by ± 0.4 GeV adjusts curves by up to $\pm 50\%$.

Points: lattice data.

Curves: dispersion relation + model for cross section.

$\mathcal{M}_{TT}$: dependence on ν and m_π

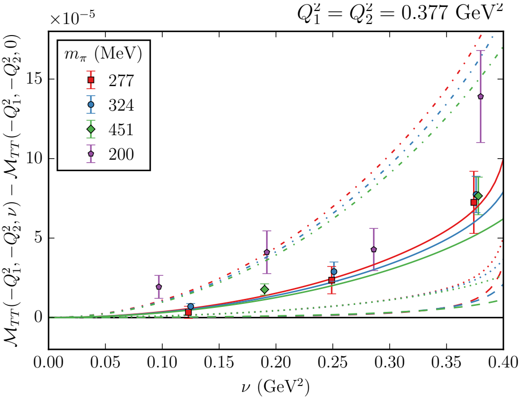

Points: lattice data.

Curves: dispersion relation + model for cross section.

In increasing order:

- π^0
- $\pi^0 + \eta'$
- full model
- full model + high-energy $\sigma(\gamma\gamma \to \text{hadrons})$ at physical m_π

Eight forward-scattering amplitudes

V. M. Budnev, V. L. Chernyak and I. F. Ginzburg, Nucl. Phys. B **34**, 470 (1971)

V. M. Budnev, I. F. Ginzburg, G. V. Meledin and V. G. Serbo, Phys. Rept. **15**, 181 (1975)

$$\begin{aligned}
\mathcal{M}^{\mu'\nu',\mu\nu}(q_1,q_2) = {} & R^{\mu\mu'}R^{\nu\nu'}\mathcal{M}_{TT} \\
& + \tfrac{1}{2}\left[R^{\mu\nu}R^{\mu'\nu'} + R^{\mu\nu'}R^{\mu'\nu} - R^{\mu\mu'}R^{\nu\nu'}\right]\mathcal{M}^{\tau}_{TT} \\
& + \left[R^{\mu\nu}R^{\mu'\nu'} - R^{\mu\nu'}R^{\mu'\nu}\right]\mathcal{M}^{a}_{TT} \\
& + R^{\mu\mu'}k_2^{\nu}k_2^{\nu'}\mathcal{M}_{TL} + k_1^{\mu}k_1^{\mu'}R^{\nu\nu'}\mathcal{M}_{LT} + k_1^{\mu}k_1^{\mu'}k_2^{\nu}k_2^{\nu'}\mathcal{M}_{LL} \\
& - \left[R^{\mu\nu}k_1^{\mu'}k_2^{\nu'} + R^{\mu\nu'}k_1^{\mu'}k_2^{\nu} + (\mu\nu \leftrightarrow \mu'\nu')\right]\mathcal{M}^{a}_{TL} \\
& - \left[R^{\mu\nu}k_1^{\mu'}k_2^{\nu'} - R^{\mu\nu'}k_1^{\mu'}k_2^{\nu} + (\mu\nu \leftrightarrow \mu'\nu')\right]\mathcal{M}^{\tau}_{TL},
\end{aligned}$$

where R is a projector onto transverse polarizations and k_a are longitudinal polarization vectors.

Eight forward-scattering amplitudes: data

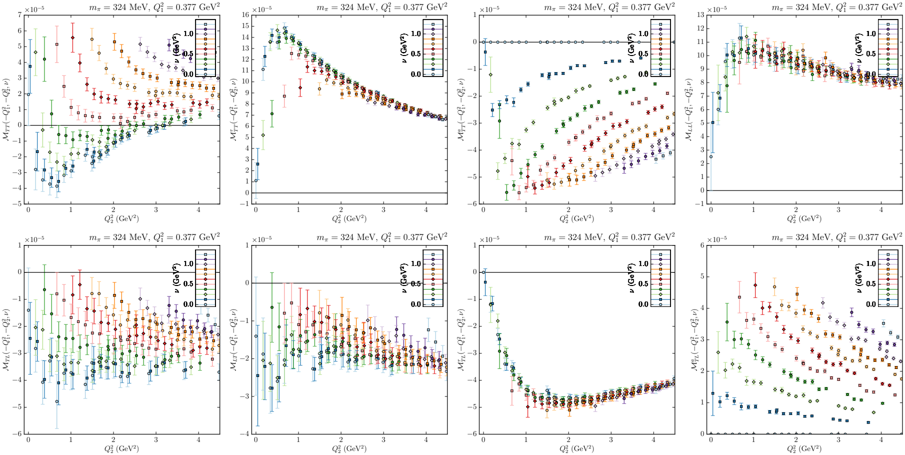

Quark contractions: relative importance

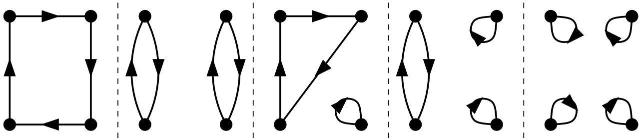

Consider the charge factors, with $q_u = 2/3$, $q_d = q_s = -1/3$:

diagram	factor	$N_f = 2$	$N_f = 3$
(4)	$\sum_f q_f^4$	17/81	18/81
(2,2)	$(\sum_f q_f^2)^2$	25/81	36/81
(3,1)	$(\sum_f q_f^3)(\sum_f q_f)$	7/81	0
(2,1,1)	$(\sum_f q_f^2)(\sum_f q_f)^2$	5/81	0
(1,1,1,1)	$(\sum_f q_f)^4$	1/81	0

It is also argued that with only the fully-connected diagrams, the η' falsely appears with the mass of the pion, so that effectively the π^0 contribution is enhanced by a factor of 34/9. J. Bijnens, J. Relefors, JHEP **1609**, 113 (2016)

(2,2) quark-disconnected contractions

Evaluate one of the quark loops using stochastic estimation.
Need the following propagators:

- 1 point-source propagator from $x_3 = 0$
- 1 noise-source propagator
- 1 noise-momentum-source propagator

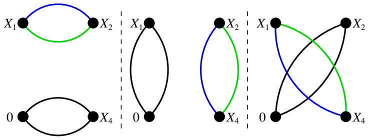

Preliminary results for unsubtracted $\mathcal{M}_{TT}$: Large finite-volume effect!

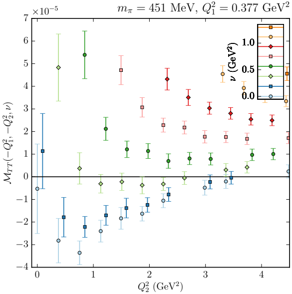

fully-connected

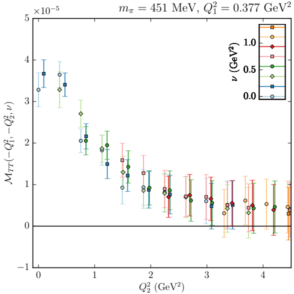

(2,2)-disconnected

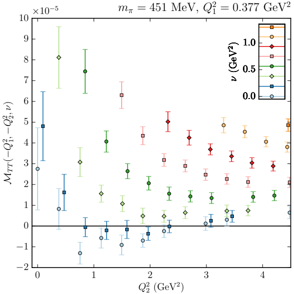

sum

(2,2) quark-disconnected contractions

Evaluate one of the quark loops using stochastic estimation.
Need the following propagators:

- 1 point-source propagator from $x_3 = 0$
- 1 noise-source propagator
- 1 noise-momentum-source propagator

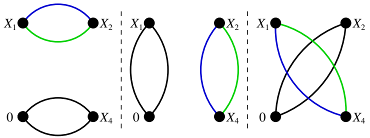

Preliminary results for subtracted $\mathcal{M}_{TT}$:

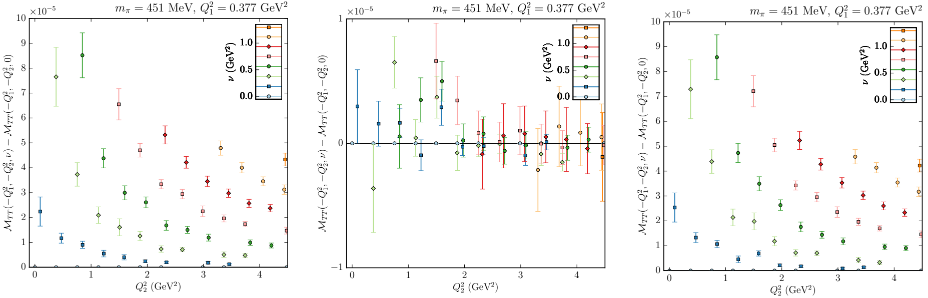

fully-connected | (2,2)-disconnected | sum

Strategy for muon $g-2$: kernel

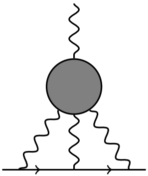

In Euclidean space, give muon momentum $p = im\hat{\epsilon}$, $\hat{\epsilon}^2 = 1$.
Apply QED Feynman rules and isolate $F_2(0)$; obtain

$$a_\mu^{\text{HLbL}} = \int d^4x\, d^4y\, \mathcal{L}_{[\rho,\sigma];\mu\nu\lambda}(\hat{\epsilon},x,y) i\hat{\Pi}_{\rho;\mu\nu\lambda\sigma}(x,y),$$

where $$\hat{\Pi}_{\rho;\mu\nu\lambda\sigma}(x_1,x_2) = \int d^4x_4\, (ix_4)_\rho \left\langle J_\mu(x_1) J_\nu(x_2) J_\lambda(0) J_\sigma(x_4) \right\rangle.$$

The integrand for a_μ is a scalar function of 5 invariants: x^2, y^2, $x\cdot y$, $x\cdot\epsilon$, and $y\cdot\epsilon$, so 3 of the 8 dimensions in the integral are trivial.
Five dimensions is still too many. Result is independent of $\hat{\epsilon}$, so we can eliminate it by averaging in the integrand:

$$\mathcal{L}(\hat{\epsilon},x,y) \to \bar{\mathcal{L}}(x,y) \equiv \langle \mathcal{L}(\hat{\epsilon},x,y)\rangle_{\hat{\epsilon}}$$

Then the integrand depends only on x^2, y^2, and $x\cdot y$.

Test of position-space kernel: π^0 contribution

N. Asmussen, JG, H. B. Meyer, A. Nyffeler, 1609.08454

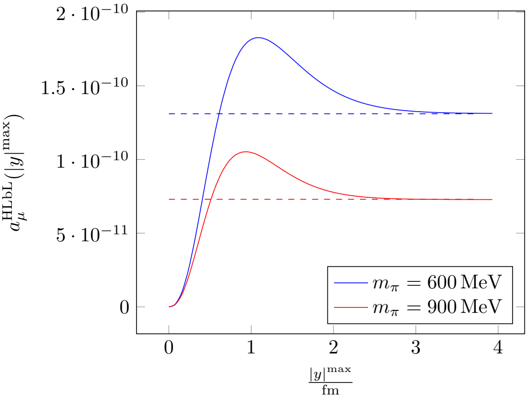

- Using a VMD model for $\mathcal{F}_{\pi^0\gamma^*\gamma^*}$, work out the π^0-exchange contribution to $\hat{\Pi}(x,y)$.
- Integrate it with the kernel $\bar{\mathcal{L}}(x,y)$ to compute $a_\mu^{\mathrm{HLbL},\pi^0}$, using a cutoff $|x|^{\max} = 4.05$ fm and varying $|y|^{\max}$.
- Compare against the result computed in momentum space.

Strategy for muon $g-2$: lattice

$$
\begin{aligned}
a_\mu^{\text{HLbL}} &= \int d^4x \int d^4y\, d^4z\, \bar{\mathcal{L}}_{[\rho,\sigma];\mu\nu\lambda}(x,y)(-z)_\rho \left\langle J_\mu(x) J_\nu(y) J_\lambda(0) J_\sigma(z) \right\rangle \\
&= 2\pi^2 \int_0^\infty x^3 dx \int d^4y\, d^4z\, \bar{\mathcal{L}}_{[\rho,\sigma];\mu\nu\lambda}(x,y)(-z)_\rho \left\langle J_\mu(x) J_\nu(y) J_\lambda(0) J_\sigma(z) \right\rangle .
\end{aligned}
$$

Evaluate the y and z integrals in the following way:

1. Fix local currents at the origin and x, and compute point-source propagators.
2. Evaluate the integral over z using sequential propagators.
3. Contract with $\bar{\mathcal{L}}_{[\rho,\sigma];\mu\nu\lambda}(x,y)$ and sum over y.

The above has similar cost to evaluating scattering amplitudes at fixed p_1,p_2.
Do this several times to perform the one-dimensional integral over $|x|$.

Summary and outlook

- Significant progress is being made in lattice QCD calculations aiming to reduce the leading theoretical uncertainties of the muon $g-2$.
- The contribution from the fully-connected four-point function to the light-by-light scattering amplitude can be efficiently evaluated if two of the three momenta are fixed.
- Forward-scattering case is related to $\sigma(\gamma^*\gamma^* \to \text{hadrons})$; lattice is consistent with phenomenology, within the latter's large uncertainty.
- For typical Euclidean kinematics the π^0 contribution is not dominant.
- We have a position-space kernel for computing the leading-order HLbL contribution to the muon $g-2$.
  Work is ongoing to integrate it into a lattice calculation.
- Phenomenology indicates the π^0 contribution is dominant for $g-2$; reaching this regime (physical m_π, large volumes) may be challenging on the lattice.
- In the meantime, calculations of the $\pi^0 \to \gamma^*\gamma^*$ form factor should improve the reliability of phenomenological values for a_μ^{HLbL}.